CHROMBIO. 2956

# EQUILIBRIUM AND RATE CONSTANTS OF IMMOBILIZED CONCANAVALIN A DETERMINED BY HIGH-PERFORMANCE AFFINITY CHROMATOGRAPHY

DAVID J. ANDERSON and RODNEY R. WALTERS*

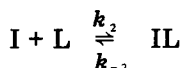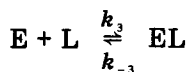*Department of Chemistry, Iowa State University, Ames, IA 50011 (U.S.A.)*

SUMMARY

Equilibrium constants for the binding of p-nitrophenyl α-D-mannopyranoside, 4-methylumbelliferyl α-D-mannopyranoside, and methyl α-D-mannopyranoside to immobilized concanavalin A were determined by high-performance affinity chromatography. Values obtained by zonal and frontal analysis on columns of variable concanavalin A coverage were in close agreement and were approximately two-fold greater than literature values from solution studies. The immobilized concanavalin A appeared to have only a slight heterogeneity. Sugars containing aromatic groups were found to be non-specifically adsorbed, but the retention was small under the conditions used for equilibrium and rate constant measurements. Dissociation rate constants for two of the sugars were determined by isocratic elution. Apparent changes in the rate constants with capacity factor were found to be due to errors in calculating the diffusional contributions to band-broadening as a function of retention. The more accurate low retention time data gave rate constants that were approximately one half of literature values.

INTRODUCTION

One application of high-performance affinity chromatography (HPAC) is the determination of kinetic and thermodynamic parameters of ligand—macromolecule complexes. The theory for the determination of equilibrium constants is well known [1—4]. For the case of reversed-role affinity chromatography, in which a macromolecule (L) is immobilized and a solute (E) is isocratically eluted using a competing inhibitor (I) in the mobile phase, the reactions of interest are:

$$E + L \underset{k_{-3}}{\overset{k_3}{\rightleftarrows}} EL$$

$$I + L \underset{k_{-2}}{\overset{k_2}{\rightleftarrows}} IL$$

$$K_3 = \frac{\{EL\}}{[E]\{L\}} = \frac{k_3}{k_{-3}} \tag{1}$$

$$K_2 = \frac{\{IL\}}{[I]\{L\}} = \frac{k_2}{k_{-2}} \tag{2}$$

where $K_2$ and $K_3$ are the binding constants, $k_2$ and $k_3$ are the association rate constants, and $k_{-2}$ and $k_{-3}$ are the dissociation rate constants [4—7]. The accolades represent surface concentration. $K_2$ and $K_3$ can be determined from the slope and intercept of a plot of $1/k'$ vs. [I]:

$$\frac{1}{k'} = \frac{V_m}{K_3 m_L} + \frac{V_m K_2[I]}{K_3 m_L} \tag{3}$$

where $k'$ is the capacity factor, $V_m$ is the column void volume, and $m_L$ is the number of moles of active ligand in the column [6, 7].

The theory for the determination of kinetic parameters is also well known [4, 5, 8—10], but few experimental studies have been performed. Although several studies of band-broadening by kinetic processes have been published [11—14] only Muller and Carr [6] have made a thorough examination of the problem. They obtained rate constants which were much lower than expected from solution studies and which varied with $k'$ in contradiction of theory [6]. In this paper the same biochemical system consisting of immobilized concanavalin A (Con A) with various sugars used as the analyte or inhibitor will be reexamined, but with changes in the support material, immobilization method, and calculation methods.

To determine dissociation rate constants, other contributions to band-broadening in the column must be negligible or be separately determined and subtracted off. The total plate height, $H$, is believed to obey the Van Deemter equation [4, 5, 8, 9, 15, 16]:

$$H = H_m + H_{sm} + H_k \tag{4}$$

where

$$H_{sm} = \frac{2u V_p (1 + V_m k'/V_p)^2}{k_{-1} V_m (1 + k')^2} \tag{5}$$

and

$$H_k = \frac{2u k'}{k_{-3}(1 + k')^2} \tag{6}$$

In eqn. 4 it is assumed that $H_m$, the eddy diffusion and mobile phase mass transfer term, is independent of $k'$ and flow-rate, and that longitudinal diffusion is negligible [15, 16]. $V_p$ is the pore volume of the column, $u$ is the linear velocity of the mobile phase, $H_{sm}$ is the contribution to the plate height due to slow diffusion in the stagnant mobile phase of the pores, and $H_k$ is the contribution due to slow adsorption—desorption kinetics. The diffusional rate constants $k_1$ and $k_{-1}$ are related to the support properties [4] through the following equation:

$$\frac{k_1}{k_{-1}} = \frac{V_p}{V_e} \tag{7}$$

where $V_e$ is the exclusion volume of the column. Also,

$$k_{-1} = \frac{60\gamma D_m}{d_p^2}$$

where $\gamma$ is a tortuosity factor, $D_m$ is the diffusion coefficient of the solute and $d_p$ is the particle diameter [8, 17, 18]. There is currently some controversy over the flow-rate and $k'$ dependence of $H_m$ and $H_{sm}$ [15, 16, 19] and surface diffusion has been postulated to be important in some cases [19].

Rate parameters can also be calculated directly from peak variances [4, 5, 8—10]. The appropriate equations, in (units of time)$^2$, are obtained by multiplying eqns. 4—6 by $t_m^2 (1 + k')^2/L$ where $t_m$ is the void time and $L$ is the column length.

EXPERIMENTAL

*Reagents*

Concanavalin A (types IV and V), p-nitrophenyl α-D-mannopyranoside (PNPM), 4-methylumbelliferyl α-D-mannopyranoside (MUM), methyl α-D-mannopyranoside (MDM, grade III), p-nitrophenyl α-D-galactopyranoside (PNPG), and 4-methylumbelliferyl α-D-galactopyranoside (MUGA) were obtained from Sigma (St. Louis, MO, U.S.A.). The Con A was purified as described previously [7]. The Hypersil WP-300, 5-$\mu$m silica and the LiChrospher SI 500, 10-$\mu$m silica were from Alltech (Deerfield, IL, U.S.A.). Carboxylate microspheres, 0.1 $\mu$m, were from Polysciences (Warrington, PA, U.S.A.).

*Apparatus*

In addition to the high-performance liquid chromatographic equipment previously described [7], a differential refractometer (Model R401, Waters Assoc., Milford, MA, U.S.A.) was used for break-through curves with MDM.

*Procedure*

Diol-bonded LiChrospher SI 500 and Hypersil 300 matrices were prepared according to a published procedure [20]. Con A was coupled to LiChrospher SI 500 diol using the 1,1'-carbonyldiimidazole method [7]. Low- and high-coverage Hypersil 300 columns were prepared by the Schiff base method using 4 ml of 3.7 mg/ml Con A or 25 ml of 9.8 mg/ml Con A per 0.8 g support [18, 21]. The pH 5 acetate buffer described below was used for the immobilization. The immobilized Con A on the LiChrospher support was assayed by the method of Lowry et al. [22].

The chromatographic columns were thermostated at 25.0°C. The mobile phase was 0.5 $M$ sodium acetate, 1 m$M$ calcium chloride and manganese chloride, pH 5.0. The inhibitor was MDM dissolved in this buffer. Sugars injected into the columns were also prepared in the appropriate MDM-containing buffer. Injection volumes of 6 $\mu M$ sugar were 20 $\mu$l for the LiChrospher affinity col-

umn and 10 $\mu$l for all other columns. The detection wavelength was 305 nm for PNPM and PNPG, 316 nm for MUM and MUGA, and 280 nm for carboxylate microspheres, uracil, and water. Flow-rates were measured volumetrically. Statistical moments were determined from the width-at-half-height and peak-center-at-half-height using a Gaussian approximation (see also eqn. 15).

Column void time ($t_m$) was determined by injection of water. Using the non-Con A-binding sugars PNPG and MUGA [23], a non-specific retention time ($t_{ns}$) was measured. The exclusion volume ($V_e$) was obtained by injection of the carboxylate microspheres diluted to a concentration of 0.25% and injected onto diol-bonded silica columns in a deionized water mobile phase to prevent agglomeration. The volume $V_e$ was assumed to be the same for the corresponding affinity column.

Extra-column void time and variance were measured without a column and subtracted from the raw retention times and peak variances. A weak non-specific retention of the sugars ($k'$ ca. 0.2) was subtracted when appropriate in the calculations. This correction had only a minor effect on the results.

In addition to zonal analysis, equilibrium constant data were obtained from some of the columns by frontal analysis. Flow-rates for the break-through studies were between 0.05 and 1 ml/min and were chosen to minimize error in estimating the break-through points. The break-through points were found by integration [24]. Uracil break-through curves were used to correct for the column void volume. The number of moles of active ligand in the column was also found using the break-through curves.

Table I lists the columns used in this study and some of the important measured parameters.

TABLE I

COLUMN PARAMETERS

| Column | Support | $L^*$ (mm) | $F$ (ml/min) | $V_m$ (ml) | $V_e$ (ml) | $m_L$ (nmol) | $\{L\}^{**}$ (nmol/m$^2$) |
|---|---|---|---|---|---|---|---|
| Diol | LiChrospher SI 500 | 49.6 | — | 0.58 | 0.25 | — | — |
| Diol | Hypersil 300 | 50.0 | — | 0.42 | 0.23 | — | — |
| Low-coverage Con A | Hypersil 300 | 50.0 | 1.00 | 0.42 | 0.23 | 16 | 0.7 |
| Medium-coverage Con A | LiChrospher SI 500 | 100.0 | 0.92 | 0.94 | 0.38 | 290 | 12 |
| High-coverage Con A | Hypersil 300 | 49.7 | 1.01 | 0.41 | 0.23 | 650 | 29 |

$^*$ All columns were 4.1 mm I.D. except the LiChrospher SI 500 diol column which was 4.6 mm I.D.
$^{**}$ Surface coverage of binding sites based on experimental packing densities and manufacturers' estimates of surface area.

RESULTS AND DISCUSSION

*Verification of linear elution conditions*

A critical parameter in experimental design is the sample size. Under linear elution conditions, the data should be independent of sample size. If this is not the case, then the theoretical relationships given earlier will not apply. Since affinity columns contain relatively few adsorption sites, overloading is a common problem. In this work, the low-coverage Hypersil 300 column was the most easily overloaded. Linear elution conditions were established by in-
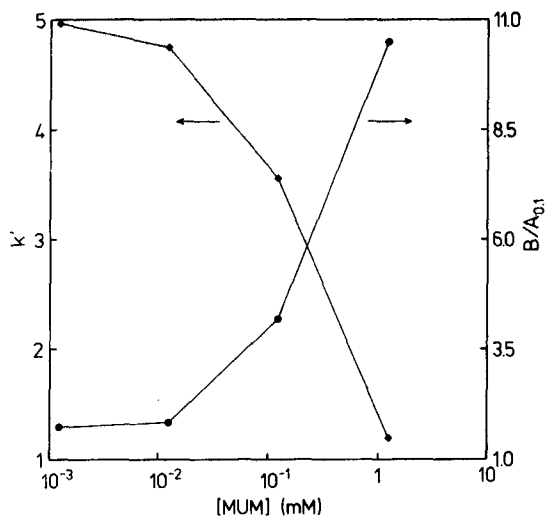
Fig. 1. Effect of sample concentration on the capacity factor $k'$ (♦) and peak asymmetry (●). Samples of MUM (10 $\mu$l) were injected onto the low-coverage Hypersil 300 column.

jecting various concentrations of MUM and measuring the capacity factor and peak asymmetry (Fig. 1). Large changes in these parameters were seen at high concentration, but the concentration used in our work (6 $\mu M$) was within the linear elution region and corresponded to filling 3% of the available sites in the worst case.

*Determination of equilibrium constants by zonal analysis*

Equilibrium constants for the solutes MUM and PNPM and the inhibitor MDM were determined from plots of eqn. 3 using the $V_m$ and $m_L$ data from Table I. The plots (Fig. 2) exhibited excellent linearity. The results (Table II)
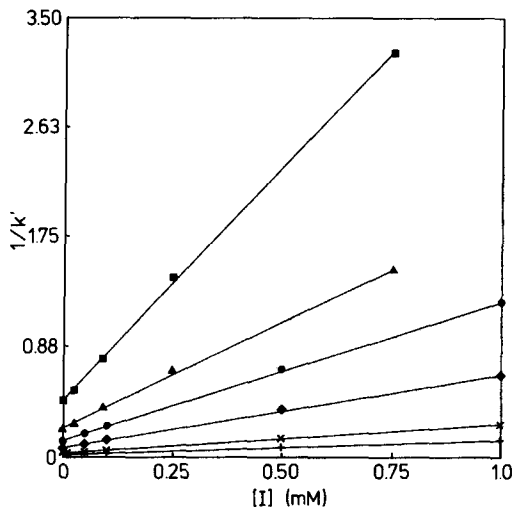


Fig. 2. Plots used to determine equilibrium constants for MUM on the high- (+), medium- (♦), and low-coverage (▲) columns and PNPM on the high- (×), medium- (●), and low-coverage (■) columns.

TABLE II

EQUILIBRIUM CONSTANT DATA

| Source | Analysis | $K_3$ (MUM) $(M^{-1})$ | $K_3$ (PNPM) $(M^{-1})$ | $K_2$ (MDM)* $(M^{-1})$ |
|---|---|---|---|---|
| Low-coverage Hypersil 300 | Zonal | 117 000** | 59 000** | 7400, 8400 |
| Medium-coverage LiChrospher SI 500 | Zonal | 45 000 | 25 000 | 8100, 8500 |
| High-coverage Hypersil 300 | Zonal | 45 000 | 22 000 | 8400, 8100 |
| Solution data [25] | — | | 33 000 | 8700 | 3300 |
| Muller and Carr [6] | Both | — | 16 000 | 7600 |
| Medium-coverage LiChrospher SI 500 | Frontal | — | 26 000 | — |
| High-coverage Hypersil 300 | Frontal | — | — | 8400 |

*First value from MUM data, second from PNPM data.

**Possible error in $m_L$ determination on low-coverage column (see text).

are higher than literature values from solution measurements by factors of 1.4- to 2.7-fold but in good agreement with the results of Muller and Carr [6]. The differences from solution values may be due to the fact that on the column $K_3$ and $K_2$ are defined in terms of surface concentrations (eqns. 1 and 2) which may not be equivalent to the solution concentrations obtained by dissolving the same number of moles in a volume $V_p$. Equilibrium constants have been measured for many other affinity chromatographic systems and have yielded values typically within a factor of two higher or lower than literature values [1—3, 13, 14]. Thus, such differences may be due to errors in the solution data.

*Determination of equilibrium constants and number of sites by frontal analysis*

Although the data in Fig. 2 were of excellent linearity, at higher inhibitor concentrations some negative deviation from the expected line was observed. This indicated some heterogeneity of the immobilized Con A and was also observed by Muller and Carr [6]. The extent of the heterogeneity appeared to be minor. For example, under conditions where only 0.2% of the Con A sites were free, the measured $k'$ value deviated by just 30% from the value expected using the higher $k'$ data.

In addition to this slight heterogeneity of the specific sites, there appeared to be a population of non-specific sites since MUGA and PNPG were slightly retained ($k' = 0.22$ and 0.10, respectively) on the affinity columns while MUM and PNPM were slightly retained ($k' = 0.27$ and 0.07, respectively) on the diol columns. This weak retention was subtracted when Fig. 2 was made and thus should not have affected the zonal data. The effect on frontal data was more severe, however.

Break-through curves were obtained for various concentrations of PNPM on the LiChrospher SI 500 column (Fig. 3a) and MDM on the high-coverage Hypersil 300 column (Fig. 3b). Using eqn. 1 the following equation was derived:

$$m_{EL} = K_3[E] m_L / (1 + K_3[E]) \tag{9}$$

where $m_{EL}$ is the number of moles of sugar bound, $m_L$ is the total number of free and occupied sites, and [E] is the concentration of sugar applied. This equation defines the well known Langmuir isotherm.
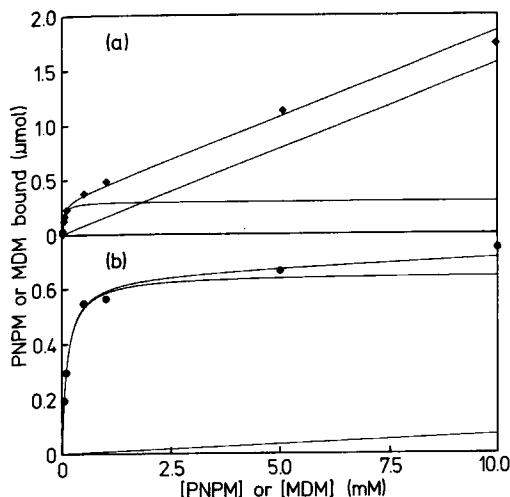
Fig. 3. Binding isotherms from break-through curves for PNPM on the LiChrospher SI 500 column (a) and for MDM on the high-coverage Hypersil 300 column (b). In each case the upper curve is the total fit to the experimental data, the straight line is the non-specific binding, and the remaining curve is the specific binding.

The PNPM experimental data in Fig. 3a did not level off at high concentrations of sugar as had been expected from the binding constants in Table II. This same behavior can be seen in the data of Muller and Carr [6] but they did not use sufficiently high sugar concentrations to make this trend obvious.

If there is a second group of non-specific sites of amount $m_{ns}$ and binding constant $K_{ns}$, then the amount bound will be:

$$m_{EL} + m_{E_{ns}} = \frac{K_3[E] m_L}{1 + K_3[E]} + \frac{K_{ns}[E] m_{ns}}{1 + K_{ns}[E]} \tag{10}$$

If it is further assumed that these are weak sites so that $K_{ns}[E] \ll 1$ over the range of [E] studied, then

$$m_{EL} + m_{E_{ns}} = \frac{K_3[E] m_L}{1 + K_3[E]} + K_{ns}[E] m_{ns} \tag{11}$$

This equation predicts the linear increase in the amount bound at high concentrations of sugar, as was seen in Fig. 3a.

Fitting our data to eqn. 11 yielded the number of moles of active sites (Table I, high- and medium-coverage columns) and the frontal analysis equilibrium constants in Table II. The latter were in excellent agreement with the zonal data and thus supported the conclusion that there was a population of weak sites on either the support or hydrophobic residues on the Con A itself, which affected the retention primarily at high sugar concentrations. The value of $K_{ns}m_{ns}$ for PNPM determined from the fit of Fig. 3a was $1.6 \cdot 10^{-4}$ $L$, which is 50-fold smaller than the value of $K_3 m_L$, $7.3 \cdot 10^{-3}$ $L$. On the high-coverage Hypersil 300 column, $K_{ns}m_{ns}$ for the sugar MDM was only $6.8 \cdot 10^{-6}$ $L$ (Fig. 3b), which suggested that PNPM was retained non-specifically via the hydrophobic phenyl group. MDM was thus more suitable for determining $m_L$.

The LiChrospher SI 500 protein content can be used to calculate a maximum value of $m_L$ of 290 nmol (based on 1 mol of sites per 27 000 g Con A, i.e., the molecular weight of a monomer [26]). This can be compared to the isotherm value in Table I (290 nmol) and indicates complete retention of activity of carbonyldiimidazole-immobilized Con A. Muller and Carr [6] observed a 50% retention of activity using the glutaraldehyde coupling method.

For the low-coverage Hypersil 300 column, $m_L$ was determined by a single break-through curve using $2.0 \cdot 10^{-3}$ $M$ MDM. The small break-through volume could not be measured accurately, so the errors in the $K_3$ values in Table II were probably due to inaccuracies in $m_L$. Note that this error would not affect the $K_2$ values.

The above discussion does not rule out the possibility of a subpopulation of very strong sites, although the data of Fig. 2 do not indicate the presence of a significant number of stronger sites. Muller and Carr [6] hypothesized the presence of such sites after plotting their frontal analysis data as a Scatchard plot. Similar plots of our isotherm data were less clear. While the weak sites discussed above were clearly seen, the presence of strong sites was less apparent because few data points were taken in the low concentration region. In the LiChrospher SI 500 data there was some indication of a small proportion (ca. 10%) of stronger sites ($K_3$ ca. $2 \cdot 10^5$ $M^{-1}$) but the data were not conclusive.

*Determination of rate constants*

In order to calculate rate parameters, we must assume that the processes involved are fairly homogeneous. With regard to the previous discussion of heterogeneity, two assumptions will be made. First, we will assume that within the range of $k'$ data in Fig. 2, the Con A is of a homogeneous nature. Data from the non-linear low $k'$ regions of these plots will not be used to calculate rate constants. Secondly, we will assume that the weak non-specific retention of sugars is kinetically fast and does not contribute to the kinetic band-broadening.

Fig. 4 shows theoretical plots of the plate height terms and variances from eqns. 4—6 (with $H_m = 0$), and experimental data. The kinetic plate height, $H_k$, always has a maximum at $k' = 1$. Combined with the $H_{sm}$ term, a maximum in the $H_{tot}$ plot is expected in the range of $k' = 1$—2. This was seen for the two Hypersil 300 columns but was less apparent for the LiChrospher SI 500 column, suggesting that kinetic band-broadening was less important than diffusional band-broadening on that column. Variance plots are shown in Fig. 4c and d. The kinetic contribution increases linearly while the diffusional contribution increases via a squared term. From the experimental data (Fig. 4d) it was difficult to visually assess the relative importance of diffusional and kinetic band-broadening. Clearly, from Fig. 4a and c, it is easier to measure adsorption—desorption kinetic parameters at low $k'$ where the diffusional contribution is smaller.

Muller and Carr [6] calculated $k_{-3}$ in two ways. First, they simply subtracted the plate height for a non-binding sugar from the total plate height for a retained sugar. This was clearly incorrect since $H_{sm}$ increases greatly with $k'$. In a second method, they used literature data to estimate various plate height
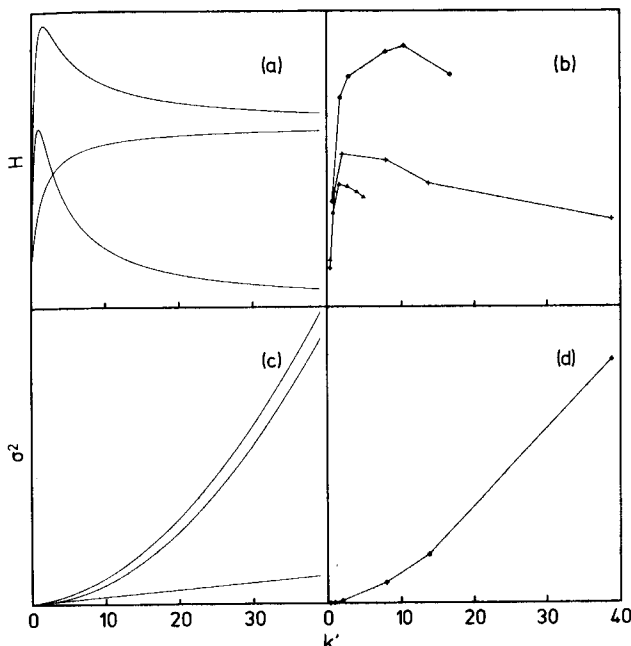
Fig. 4. Theoretical and experimental plots of plate height (a and b) and variance (c and d) vs. $k'$. (a and c) From top to bottom: total, diffusional, and kinetic contributions to the plate height and variance calculated from eqns. 5 and 6. (b) Experimental data for MUM on the high-coverage Hypersil 300 (+), medium-coverage LiChrospher SI 500 (♦), and low-coverage Hypersil 300 (▲) columns. (d) Data for MUM on the high-coverage Hypersil 300 column.

contributions. Both approaches yielded similar results: the non-kinetic contributions were small compared to the total plate height, thus $H_k$ was assumed to dominate. In support of this they showed that the band-broadening on a 50-$\mu$m support was only five-fold greater than on a 10-$\mu$m support rather than the expected 25-fold change if $H_{sm}$ were dominant.

We similarly saw a two-fold reduction in plate height as the particle diameter decreased from 10 to 5 $\mu$m (Fig. 4b) rather than the expected four-fold change if $H_{sm}$ dominated. In addition, plate heights on the LiChrospher SI 500 support (ca. 1000 $\mu$m) were similar to those observed by Muller and Carr [6] on the same support. Thus, their raw data were similar to ours, but we have looked at the data somewhat differently. We believe that diffusional contributions were much larger than indicated by Muller and Carr's work [6].

*Independent estimation of $H_{sm}$ and $H_m$*

If eqn. 4 is an accurate representation of the band-broadening in a column, then a non-retained solute will have contributions from only $H_m$ and $H_{sm}$. By measuring $H$ vs. $u$ for PNPM and MUM on a diol column (or, alternatively, PNPG and MUGA on an affinity column), one should be able to obtain $k_{-1}$ from the slope and $H_m$ from the intercept. This is shown in Fig. 5 for the case of MUM on a LiChrospher SI 500 diol column. Such plots were generally quite linear, thus indicating good agreement with the Van Deemter equation. Table III summarizes the results. Similar results were obtained for MUGA and PNPG
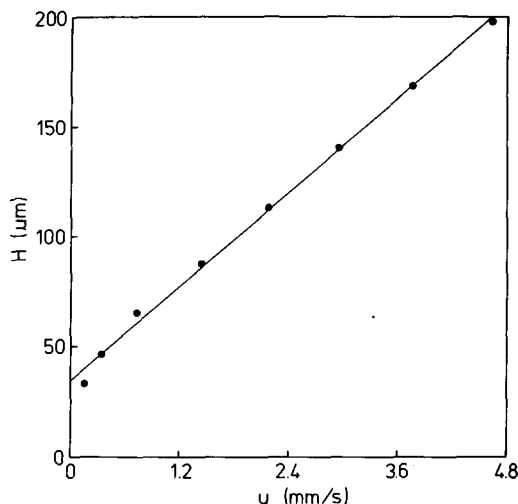
Fig. 5. Plate height for MUM on the LiChrospher SI 500 diol column as a function of linear velocity.

TABLE III

DIFFUSIONAL PARAMETERS

| Column | Sugar | $H_m$ ($\mu$m) | $k_{-1}$ (s$^{-1}$) |
|---|---|---|---|
| LiChrospher SI 500 diol | MUM | 34 | 43 |
| | PNPM | 33 | 78 |
| Hypersil 300 diol | MUM | 28 | 116 |
| | PNPM | 30 | 123 |
| Low-coverage Hypersil 300 | MUGA | 19 | — |
| | PNPG | 23 | — |
| Medium-coverage LiChrospher SI 500 | MUGA | 85 | — |
| | PNPG | 108 | — |
| High-coverage Hypersil 300 | MUGA | 25 | — |
| | PNPG | 39 | — |

on the high-coverage Hypersil 300 column. As one would expect, $k_{-1}$ was larger for the smaller support, but by less than the theoretical factor of four.

To take into account inter-column variation, $H_m$ was also determined for each affinity column using the non-retained sugars and assuming that $k_{-1}$ was the same as the similar sugar on the diol column. As shown in Table III, $H_m$ was, in most cases, of similar magnitude.

Using the values of $H_m$, $k_{-1}$, $u$, $V_m$, and $V_p$, $H_{sm} + H_m$ was calculated as a function of $k'$ and subtracted from the measured plate height of each data point. The remaining plate height was assumed to be due to $H_k$, and $k_{-3}$ was calculated for each point using eqn. 6. Fig. 6 shows the calculated values of $k_{-3}$ as a function of MDM concentration. Not only were different values of $k_{-3}$ obtained on each column, but $k_{-3}$ for the same solute differed from column to column. Muller and Carr [6] also observed that $k_{-3}$ increased as the inhibitor concentration increased. They postulated a linear dependence of $k_{-3}$ on [I]
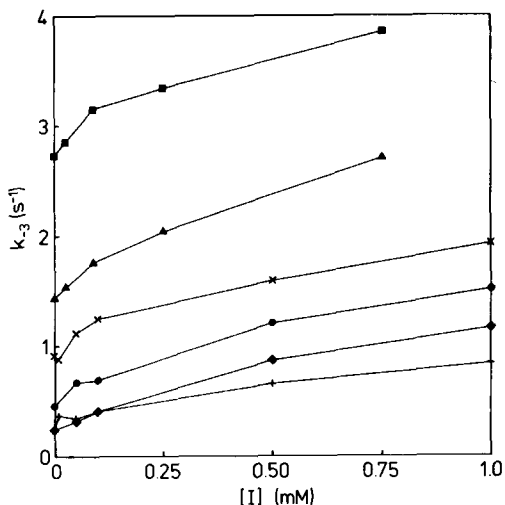
Fig. 6. Plots of the calculated dissociation rate constant versus inhibitor (MDM) concentration. Symbols are the same as in Fig. 2.

from PNPM data on a single column, but our Fig. 6 indicates that the dependence is probably not linear. Our values of $k_{-3}$ for PNPM on the LiChrospher SI 500 column were quite similar to their values using the same support.

To account for the change in $k_{-3}$ as a function of [I], Muller and Carr [6] postulated that the inhibitor altered the kinetics of the Con A—PNPM complex by forming a ternary complex intermediate. This is contrary to what one would expect, i.e., that the inhibitor simply fills some of the Con A sites but has no effect on the remaining unoccupied or PNPM-occupied sites.

If Muller and Carr's hypothesis [6] were true, then $k_{-3}$ should be the same for all of the columns for a given inhibitor concentration and solute. Fig. 6 clearly shows this not to be true.

We propose an alternative explanation. We believe that the methods used by ourselves and Muller and Carr [6] to correct for the diffusional contributions were in error because of inaccurate calculation of these terms as a function of $k'$. In this case one might expect the apparent $k_{-3}$ to be a function of $k'$ rather than [I]. Fig. 7, a plot of $k_{-3}$ vs. $1/k'$, indicates that this might be the case. (Note: $1/k'$ was plotted to make the figure more comparable to Fig. 6; the same trends were observed if $k_{-3}$ was plotted vs. $k'$.) The high- and low-coverage Hypersil column data for a given solute, which are shown connected by a dotted line, appeared to be part of a continuous data set, in agreement with our hypothesis. The $k_{-3}$ values seemed to plateau at low $k'$ at values which were close to the literature data from solution (Table IV). This suggested that the error in the diffusional corrections was worse as $k'$ increased, which would be expected since these diffusional parameters were measured at $k' = 0$.

On the other hand, the LiChrospher SI 500 data points were not on these curves and did not even show differences between MUM and PNPM (Fig. 7). Since the diffusional properties of the two supports were different, this suggested that the corrections for the LiChrospher SI 500 support were so gross-
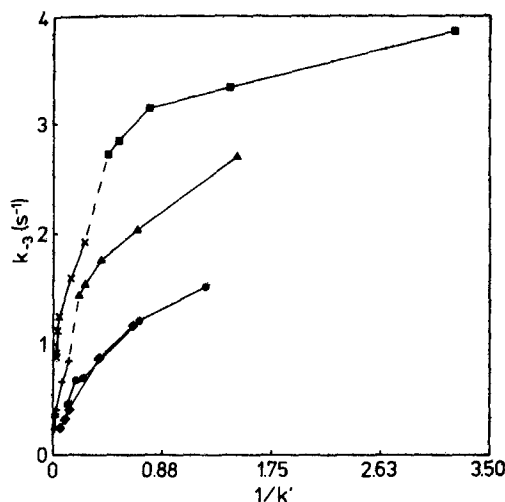
Fig. 7. Plots of the calculated dissociation rate constant ($k_{-3}$) vs. $1/k'$. Symbols are the same as in Fig. 2.

TABLE IV

RATE CONSTANT VALUES OBTAINED BY VARIOUS METHODS FROM THE LOW-COVERAGE HYPERSIL 300 COLUMN

| Method | MUM | | PNPM | |
|---|---|---|---|---|
| | $k_{-3}$ ($s^{-1}$) | $k_3{}^{\star}$ ($M^{-1}\,s^{-1}$) | $k_{-3}$ ($s^{-1}$) | $k_3{}^{\star}$ ($M^{-1}\,s^{-1}$) |
| Literature [25] | 3.4 | $11.3 \cdot 10^4$ | 6.2 | $5.4 \cdot 10^4$ |
| Visual extrapolation of Fig. 7 | 3. | $14.0 \cdot 10^4$ | 4. | $9.6 \cdot 10^4$ |
| Plate height with $H_m$ and $k_{-1}$ fixed at experimental values | 1.9 | $8.6 \cdot 10^4$ | 3.1 | $7.4 \cdot 10^4$ |
| Plate height with $H_m$ and $k_{-1}$ variable | 2.1 | $9.5 \cdot 10^4$ | 3.5 | $8.4 \cdot 10^4$ |
| Variances with $H_m$ and $k_{-1}$ fixed at experimental values | 1.5 | $6.8 \cdot 10^4$ | 2.9 | $7.0 \cdot 10^4$ |
| Variances with $H_m$ and $k_{-1}$ variable | 1.7 | $7.7 \cdot 10^4$ | 3.3 | $7.9 \cdot 10^4$ |

$^{\star}$Assuming $K_3$ = 45 000 for MUM and 24 000 $M^{-1}$ for PNPM from the HPAC data in Table II.

ly in error that differences in kinetic properties of the two solutes were no longer apparent. This might be expected since Fig. 4b showed very little apparent kinetic contribution for this support.

*Total curve-fitting approach*

The problem described above is shown more clearly in Fig. 8a. The contributions of $H_m$ and $H_{sm}$ calculated from the data in Table III obviously did not come anywhere close to accounting for the band-broadening at high $k'$ where the kinetic contribution must always be small. Thus, calculating $k_{-3}$ from the high $k'$ data invariably led to low values of $k_{-3}$.
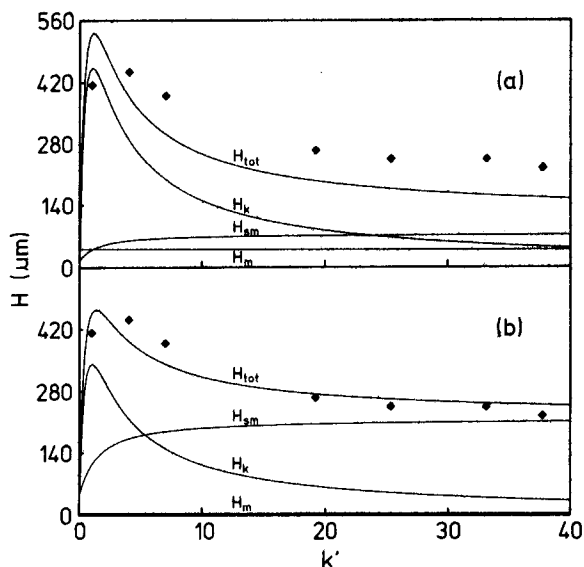
Fig. 8. Plots of plate height vs. $k'$ for the PNPM data on the high-coverage Hypersil 300 columns (♦). (a) The calculated $H_m$ and $H_{sm}$ from Table III are shown along with the best fit of $H_k$ to the remaining plate height. (b) The value of $H_{sm}$ was allowed to increase to better account for the band-broadening at high $k'$.

An alternative method is to fit an entire data set to eqn. 4. Such fits typically gave unrealistic (negative) values for $H_m$. We also did the best fit to the kinetic data after constraining $H_m$ and $k_{-1}$ to the values given in Table III. This is shown in Fig. 8a, and the fit is obviously not good. In Fig. 8b, $H_m$ and $k_{-1}$ were allowed to vary but with the constraints that $H_m$ had to be positive and that the sum of $H_m$ and $H_{sm}$ at $k' = 0$ equaled the measured value for the non-retained sugar MUGA or PNPG. This yielded somewhat better results. Similar fits using variances were also tried. Table IV summarizes some of the results for the low-coverage columns which we believe yielded the most accurate data. The values of $k_{-3}$ were somewhat smaller than literature values but were in the region expected given the somewhat larger equilibrium constants previously determined. Thus association rate constant values were similar to those measured in solution.

Although these results were reasonable, in general the curve-fitting results were unsatisfactory in that $H$ declined more slowly after peaking out than the equations predicted. Golay-type equations [15, 16] did not give any better results. The inescapable conclusion is that the chromatographic theory used here did not adequately describe the band-broadening over a wide range of $k'$. Further work is needed to examine this problem.

*Peak shape data*

In addition to the discrepancies between experimental and theoretical $H$ vs. $u$ plots, we have examined discrepancies in the peak shapes as another way of comparing experimental data with the model used to derive eqns. 5 and 6. This study also provided useful information on how to measure the statistical moments of the peaks.

Computer simulations of the stagnant mobile phase and adsorption—desorption kinetic terms were performed at various plate numbers and capacity factors using first-order rate equations.

The moment coefficient of skewness, $G_1$, is one measure of peak shape [17]. It is calculated from the second and third moments of a peak [27]. For reversed-role affinity chromatography, $G_1$ can be written as [27]:

$$G_1 = 3 \sqrt{\frac{uV_m}{2LV_p}} \cdot \frac{\dfrac{(1 + V_m k'/V_p)^3}{k_{-1}^2} + \dfrac{2V_m k'(1 + V_m k'/V_p)/V_p}{k_{-1}k_{-3}} + \dfrac{V_m k'/V_p}{k_{-3}^2}}{\left( \dfrac{(1 + V_m k'/V_p)^2}{k_{-1}} + \dfrac{V_m k'/V_p}{k_{-3}} \right)^{3/2}} \qquad (12)$$

If diffusion is very rapid, this reduces to

$$G_1 = 3 \sqrt{u/2Lk'k_{-3}} \qquad (13)$$

which shows that the peaks become more symmetric as $k'$ or $k_{-3}$ increase. If desorption is very rapid, the equation reduces to

$$G_1 = 3 \sqrt{uV_m/2V_pLk_{-1}} \qquad (14)$$

which is the same as given previously [17] and which indicates that the peak shape is independent of retention.

Various values of $k_{-1}$, $k_{-3}$, $L$, $V_p$, and $V_e$ were used to simulate peaks with $k'$ from 0 to 5, plate numbers from 2 to 100, and $V_m/V_p$ from 2 to 11. The peak skewness $(B/A_{0.1})$, a peak shape parameter that is experimentally measured more accurately than the higher statistical moments [28] but which is difficult to predict theoretically, was determined for each peak. Fig. 9 shows that there is predicted to be a direct relationship between $B/A_{0.1}$ and $G_1$ even under widely varying conditions. Plots of $B/A_{0.1}$ or $G_1$ versus plate number do
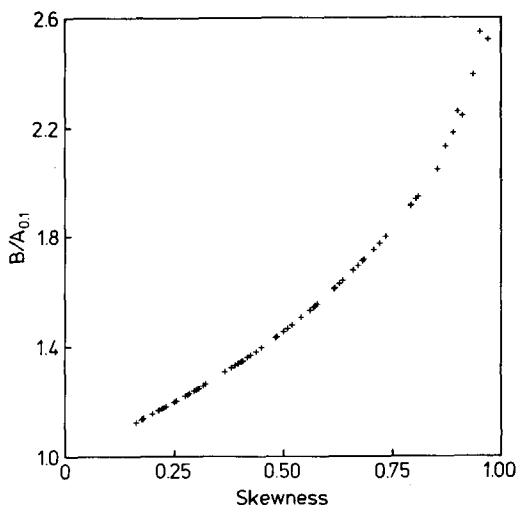


Fig. 9. Plot of the peak asymmetry from a computer simulation versus the moment coefficient of skewness calculated from eqn. 12 under a variety of conditions and assuming that only $H_{sm}$ and $H_k$ caused band-broadening. The scatter at high skewness was due to inaccuracies in the computer program.

not yield a 1:1 relationship, although there is a general improvement in symmetry as $N$ increases.

Our experimental data showed almost no change in $B/A_{0.1}$ as $k'$ changed. This is an indication that diffusional band-broadening dominated over most of the range of $k'$, as we have postulated earlier.

Plate numbers were also calculated from the width-at-half-height $(W_{0.5})$ and the peak-center-at-half-height $(V_{0.5})$:

$$N_{0.5} = 5.545 \left( \frac{V_{0.5}}{W_{0.5}} \right)^2 \tag{15}$$

It was found that $N_{0.5}$ was an excellent measure of the true plate number since the simulated peaks were generally close to Gaussian. Even under the extremes examined, $N_{0.5}$ was within $\pm 5\%$ of the true plate number in the range $N \geqslant 10$. The only exceptions were the unusual cases of split-peaks [18].

Fig. 10 compares the experimental $B/A_{0.1}$ values for the Con A columns with the simulated values at various plate numbers. It can be seen that the experimental peaks were more tailed than predicted and thus there was some
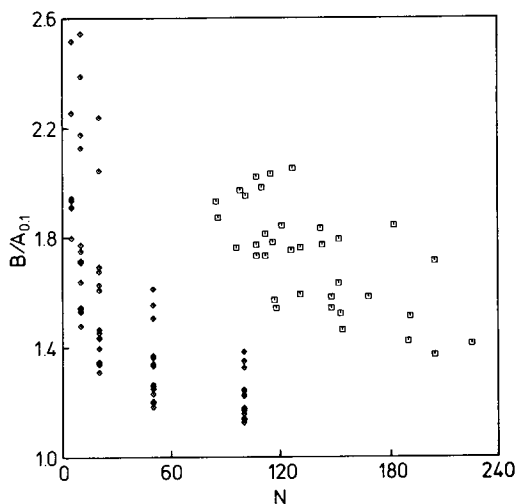


Fig. 10. Scatter diagrams showing peak asymmetries as a function of plate number from the affinity column data (□) and the computer simulations (◇).

TABLE V

EFFECT OF DIFFUSIONAL HETEROGENEITY AT $k' = 1$

| $k_{-1}$ | $N_m$ * | $N_{0.5}/N_m$ | $B/A_{0.1}$ |
|---|---|---|---|
| 0.2 (100%) | 177 | 0.99 | 1.11 |
| 0.02 (20%), 0.2 (80%) | 63 | 1.13 | 1.62 |
| 0.2 (80%), 2.0 (20%) | 216 | 0.98 | 1.12 |
| 0.02 (10%), 0.2 (80%), 2.0 (10%) | 98 | 1.18 | 1.52 |
| 0.1 (10%), 0.2 (80%), 0.4 (10%) | 169 | 0.99 | 1.13 |

*$N_m$ is the true statistical moments plate number.

discrepancy between the model and the real data. One source of such discrepancies could be heterogeneities, such as a range of particle sizes.

Table V shows the results of a simulation experiment in which diffusional heterogeneity was studied under conditions where adsorption—desorption kinetics were negligible. The column of $k_{-1}$ values indicates the percentage of particles with the given rate constant. Note that a ten-fold change in $k_{-1}$ corresponds to an approximately three-fold change in particle diameter. Commercial supports are somewhere between the values given in the last two rows of Table V. It is apparent that such heterogeneity could account for much of the peak asymmetry experimentally observed. It is also seen that there was a moderate decrease in the accuracy of $N_{0.5}$ as the peaks became less symmetric, with $N_{0.5}$ tending to overestimate the plate number. However, the errors were small compared to experimental errors often encountered in determining the true plate number by the summation method [29] and so $N_{0.5}$ was used in all the experimental data presented previously.

The diffusional heterogeneity should not affect the accuracy of the kinetic determinations because it was found that the apparent $k_{-1}$ value calculated from the peak profiles obeyed eqn. 5 exactly even when the peak shape changed. The same conclusion has been obtained theoretically [29]. However, it may be that other sources of heterogeneity not considered here might be less well behaved and could cause the non-ideal $H$ vs. $k'$ behavior.

CONCLUSIONS

While retention data appear to be adequately described by theory, kinetic data were inadequately described as a function of $k'$. Since diffusional band-broadening was significant even when small sugars were chromatographed on 5-$\mu$m supports, it is apparent that even smaller or non-porous particles are needed to accurately measure dissociation rate constants in the range of 5 s$^{-1}$. Further work is also needed to study the causes of non-ideal peak shapes and $H$ vs. $k'$ plots.

ACKNOWLEDGEMENTS

REFERENCES

1   B.M. Dunn and I.M. Chaiken, Proc. Natl. Acad. Sci. U.S.A., 71 (1974) 2382.
2   B.M. Dunn, Appl. Biochem. Biotechnol., 9 (1984) 261.
3   J. Turkova, Affinity Chromatography, Elsevier, Amsterdam, 1978, p. 35.
4   H.W. Hethcote and C. DeLisi, J. Chromatogr., 248 (1982) 183.
5   H.W. Hethcote and C. DeLisi, in I.M. Chaiken, M. Wilchek and I. Parikh (Editors), Affinity Chromatography and Biological Recognition, Academic Press, New York, 1983, p. 119.
6   A.J. Muller and P.W. Carr, J. Chromatogr., 284 (1984) 33.
7   D.J. Anderson and R.R. Walters, J. Chromatogr., 331 (1985) 1.

8  J.C. Giddings, Dynamics of Chromatography, Marcel Dekker, New York, 1965, pp. 38, 138, 244.
9  C. Horvath and H.-J. Lin, J. Chromatogr., 149 (1978) 43.
10 F.C. Denizot and M.A. Delaage, Proc. Natl. Acad. Sci. U.S.A., 72 (1975) 4840.
11 V. Kasche, K. Buchholz and B. Galunsky, J. Chromatogr., 216 (1981) 169.
12 R.R. Walters, J. Chromatogr., 249 (1982) 19.
13 K. Nilsson and P.-O. Larsson, Anal. Biochem., 134 (1983) 60.
14 I.M. Chaiken, Anal. Biochem., 97 (1979) 1.
15 E.D. Katz and R.P.W. Scott, J. Chromatogr., 270 (1983) 29.
16 E. Katz, K.L. Ogan and R.P.W. Scott, J. Chromatogr., 270 (1983) 51.
17 H.W. Hethcote and C. DeLisi, J. Chromatogr., 240 (1982) 269.
18 D.S. Hage, R.R. Walters and H.W. Hethcote, Anal. Chem., 58 (1986) in press.
19 R.W. Stout, J.J. DeStefano and L.R. Snyder, J. Chromatogr., 282 (1983) 263.
20 R.R. Walters, in P.D.G. Dean, W.S. Johnson and F.A. Middle (Editors), Affinity Chromatography: A Practical Approach, IRL Press, Oxford, 1985, p. 25.
21 P.-O. Larsson, M. Glad, L. Hansson, M.-O. Mansson, S. Ohlson and K. Mosbach, Adv. Chromatogr., 21 (1983) 41.
22 O.H. Lowry, N.J. Rosebrough, A.L. Farr and R.J. Randall, J. Biol. Chem., 193 (1951) 265.
23 I.J. Goldstein, C.E. Hollerman and E.E. Smith, Biochemistry, 4 (1965) 876.
24 U. Lund, J. Liq. Chromatogr., 4 (1981) 1933.
25 R.M. Clegg, F.G. Loontiens, A. Van Landschoot and T.M. Jovin, Biochemistry, 20 (1981) 4687.
26 A.J. Kalb and A. Lustig, Biochem. J., 109 (1968) 669.
27 H.W. Hethcote, University of Iowa, Iowa City, IA, personal communication.
28 D.J. Anderson and R.R. Walters, J. Chromatogr. Sci., 22 (1984) 353.
29 C. DeLisi, H.W. Hethcote and J.W. Brettler, J. Chromatogr., 240 (1982) 283.